ELSEVIER

Journal of Chromatography A, 813 (1998) 333–347

JOURNAL OF CHROMATOGRAPHY A

# Continuous enantiomer separation of the volatile inhalation anesthetic enflurane with a gas chromatographic simulated moving bed unit

Markus Juza[a], Orazio Di Giovanni[b], Giovanni Biressi[a], Volker Schurig[c], Marco Mazzotti[b], Massimo Morbidelli[a,*]

[a]*ETH Zürich, Laboratorium für Technische Chemie LTC, CAB C40, Universitätstrasse 6, CH-8092 Zurich, Switzerland*
[b]*ETH Zürich, Institut für Verfahrenstechnik, Sonneggstrasse 3, CH-8092 Zurich, Switzerland*
[c]*Institut für Organische Chemie, Universität Tübingen, Auf der Morgenstelle 18, D-72076 Tübingen, Germany*

Received 26 March 1998; accepted 14 April 1998

**Abstract**

The separation of the enantiomers of the racemic inhalation anesthetic enflurane was achieved by continuous gas phase simulated moving bed chromatography (GC–SMB). The productivity of the unit and the enantiomeric excess of the obtained streams were somehow low mainly because of the high operating temperature, i.e., $T=50°C$. As chiral stationary phase, an unpurified cyclodextrin derivative, consisting of various isomers and homologues and dissolved in an apolar polysiloxane matrix, was used. The competitive adsorption isotherms of (*R*)-(−)-enflurane and (*S*)-(+)-enflurane were determined by gas chromatographic measurements at increasing values of the pulse concentration in the range from linear to overload conditions. It has been shown that the adsorption behavior of the two enantiomers can be explained by considering enantioselective and non-enantioselective sites on the stationary phase. These results demonstrate the feasibility of the chiral resolution of enflurane by GC–SMB. 

*Keywords:* Enantiomer separation; Simulated moving bed chromatography; Preparative chromatography; Adsorption isotherms; Enflurane; Anesthetics; Cyclodextrin

## 1. Introduction

In view of the recent realization that the enantiomers of the volatile anesthetic isoflurane may have different or improved pharmacological properties compared to the racemate [1–6], it has become of great importance to provide sufficient amounts of the pure enantiomers for biological and medical trials and also to design a feasible process for industrial production. An isomer of isoflurane, enflurane (cf. Fig. 1) ($F_2HCOCF_2C^*HFCl$) was synthesized in 1963 by Terell [7,8]. Several advantages of this volatile chlorofluoroether over halothane, the number one inhalation anesthetic of that period, were noted.

In particular, enflurane was proved to be as stable to sunlight and to soda-lime as halothane and its metabolism was in the 2–3% range, thus about one-order of magnitude lower than that of halothane. However, its chirality was ignored at that time and only recently the synthesis of the enantiomers was described [9]. A recent study describes the enflurane metabolism for (*R*)-(−)-enflurane to be significantly

*Corresponding author.

0021-9673/98/$19.00 
PII: S0021-9673(98)00322-7

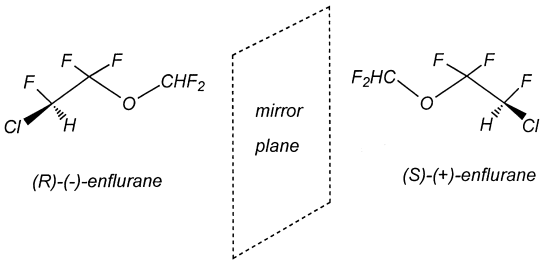


Fig. 1. The chiral inhalation anesthetic enflurane.

higher than for (*S*)-(+)-enflurane [10]. The recent developments of chiral separations by capillary gas chromatography led to the enantiomer separation of enflurane and halothane on 25 m fused-silica capillary columns coated with hexakis(2,3,6-tri-*O*-pentyl)-α-cyclodextrin and with octakis(6-*O*-methyl-2,3-di-*O*-pentyl)-γ-cyclodextrin, respectively, at 30°C [9]. It was later found that enflurane can be separated with an exceedingly high chiral separation factor, namely $\alpha > 2$, on octakis(3-*O*-butanoyl-2,6-di-*O*-*n*-pentyl)-γ-cyclodextrin [11], thus permitting the efficient preparative gas chromatographic enantiomer separation of this compound in high chemical and enantiomeric purity [12–14]. In parallel investigations, Vigh and coworkers [15–17] analytically and preparatively separated the enantiomers of enflurane on undiluted trifluoroacetylated γ-cyclodextrin, a commercially available synthetic mixture of isomers and homologues.

In this work the scale up of the batch preparative chromatography to the continuous chromatographic separation of enflurane enantiomers based on the simulated moving bed (SMB) technology is investigated. SMB is a well known technique in the field of large scale hydrocarbon separations which nowadays is attracting increasing interest for fine chemical applications, in particular for enantiomer separations using high-performance liquid chromatography (HPLC)-SMB units [18–32]. It is based on the simulation of the true counter-current (TCC) unit illustrated in Fig. 2, where the complete separation of a binary mixture consisting of a more retained and a less retained component, A and B, respectively, is considered. In the SMB unit illustrated in Fig. 3, the solid beds are fixed and the counter-current solid movement is simulated by switching the inlet and

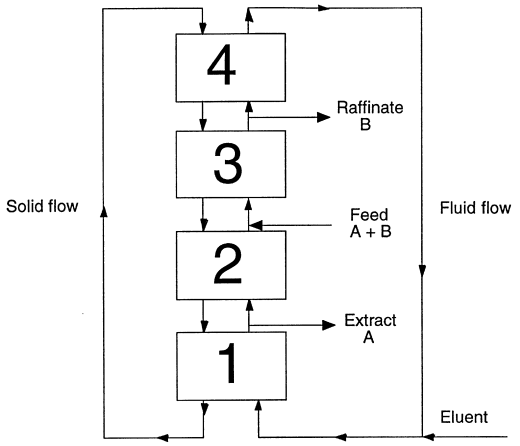


Fig. 2. Theoretical configuration: true counter-current unit.

outlet ports of the unit in the same direction as the mobile phase flow in a periodic way.

Although most applications of the SMB technology are in the liquid phase, SMBs can be operated also under supercritical conditions [33] and in the gas phase [34,35]. In comparison to other techniques, in particular batch preparative chromatography, the SMB technology has a higher separation efficiency, since smaller amounts of mobile and stationary phase are needed. Therefore it is very attractive to scale up enantiomer separations from batch preparative chro-

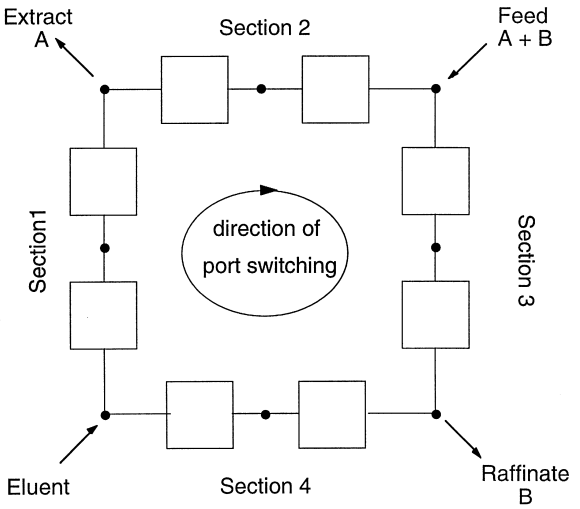


Fig. 3. Practical implementation: SMB unit.

matography to SMB using the same chiral stationary phase (CSP), also when preparative chromatography is performed in the gas phase.

The scale-up to a GC–SMB chiral separation is reported here for the first time. It is worth noting that this application exhibits several important differences with respect to previously reported non-chiral vapor phase separations [34,35]. Probably the most relevant one is that in this case the SMB application is based on elution chromatography rather than displacement chromatography. This implies that the mobile phase, i.e., the desorbent in the SMB jargon, does not interact or interacts very weakly with the CSP. Therefore, the components to be separated, i.e., the two enantiomers in this case, must be fed to the SMB unit diluted in an eluent stream; in general their mole fraction in the feed stream is rather low (a few percent in the case presented in this work). In the following, the whole development of the separation from analytical to preparative and to SMB continuous chromatography, using the same mobile phase and CSP, is demonstrated. Our results indicate that also in the case of GC, the scale-up of analytical methods to production scale chromatography may result in separation performances of practical and industrial interest.

To achieve large scale production, SMB units usually operate in overload conditions, where the adsorption behavior is competitive and non-linear. These effects must be properly accounted for in order to choose the operating conditions, i.e., flow-rates and switch time, which optimize the separation performance in terms of purity of the products, recovery and productivity [36].

## 2. Experimental

### 2.1. Materials

Racemic enflurane was obtained from the Universitätsklinik Tübingen, Abteilung für Anästhesiologie und Transfusionsmedizin. γ-Cyclodextrin was a courtesy from Wacker Chemie, Munich, Germany. Proper safety measures were applied during the whole experimental work to handle enflurane.

### 2.2. Preparation of the chiral stationary phase

#### 2.2.1. Synthesis of octakis(3-O-butanoyl-2,6-di-O-n-pentyl)-γ-cyclodextrin

A 25-g amount of octakis(3-*O*-butanoyl-2,6-di-*O*-*n*-pentyl)-γ-cyclodextrin was synthesized according to the procedure of König et al. [11], except that the acylation was accomplished in triethylamine at 50°C.

The unpurified crude product, which was only filtered over a small amount of silica gel in order to remove the catalyst and the unreacted cyclodextrin, was dried at 60°C and 0.008 Torr for 16 h (1 Torr=133.322 Pa).

Matrix-assisted laser desorption ionization time-of-flight (MALDI-TOF) mass spectra were recorded with a Bruker Reflex II MALDI-TOF system equipped with a $N_2$ laser (337 nm, 3 ns pulsewidth, 5.9 μJ) and an ion optic with ±35 kV using 20 kV source potential and delayed extraction in the linear mode. The data acquisition rate was 1 GHz, 250 spectra each were accumulated. The analytes were dissolved in $CH_2Cl_2$ (1 μg/ml) and 5–10 μl of the solutions were mixed with aliquot amounts of 0.02 mol diammonium citrate solution and the matrix (0.2 mol 2,4,6-trihydroxyacetophenone dissolved in ethanol) in a ratio of 1:5 (v/v).

#### 2.2.2. Preparation of the packing

A 96.2 g amount of polysiloxane SE-54 (WGA, Dusseldorf, Germany) was dissolved in 2000 ml dry chloroform under reflux conditions in a round-bottomed flask and 24.9 g of the γ-cyclodextrin derivative were added to the solution. A 600 g amount of Chromosorb P AW DMCS (80–100 mesh; Alltech, Arlington Heights, IL, USA) was poured into the mixture. The slurry was manually agitated until it became homogeneous. The solvent was carefully evaporated using a rotary evaporator at 40°C and a moderate vacuum for several hours followed by drying at 70°C and 0.004 Torr for 10 h. The Chromosorb prepared in this way was coated with 16.8% (w/w) of stationary phase, which consisted of 20.5% (w/w) cyclodextrin derivative dissolved in SE-54.

#### 2.2.3. Preparation of the packed columns

Before the columns were filled, the stationary phase was sieved carefully (mesh 100) to exclude

lumps and to ensure a homogenous flow through the column. One semi-preparative column made of glass (214 cm×3.9 mm I.D.) and six SMB columns made of stainless steel (120 cm×15 mm I.D.) were packed as described previously [37]. The packed beds have a plug of silanized glass wool at each end to allow a good radial distribution of the flow. The resulting adsorption bed length was 209 cm for the glass column and around 105 cm for the SMB columns.

### *2.3. Measurement of the adsorption equilibria*

The semi-preparative glass column was used to characterize the adsorption equilibria of the two enflurane enantiomers at different temperatures. It was installed in a Fractovap 4200 gas chromatograph (Carlo Erba, Milan, Italy), equipped with a flame ionization detection (FID) system. Nitrogen was used as carrier gas. The inlet pressure was measured with a manometer, while the flow-rate was measured with a soap-bubble flowmeter.

### *2.4. GC–SMB pilot unit*

The pilot unit is based on an older set-up used previously for the vapor phase separation of xylenes [34] and of linear and branched hydrocarbons [35] at temperatures around 200°C. It was modified by designing a new feeding system and a collecting system, which allows to recover enflurane from very diluted gas streams through condensation. Nitrogen was used as mobile phase, acting as diluting carrier gas for the feed stream and as eluent.

The separation section of the plant consists of four chromatographic columns, arranged in an open-loop three-section configuration [35]. The scheme of the 2–1–1 plant configuration adopted is illustrated in Fig. 4; the first section, between the eluent inlet and the extract port, is made of two columns; the second section, between the extract outlet and the feed inlet, consists of one column; the third section, between the feed inlet and the raffinate outlet, is also comprised of one column. A more detailed scheme of the whole experimental apparatus is shown in Fig. 5.

The feeding unit allowed one to choose suitable concentrations of the volatile anesthetic enflurane in the feed stream. Since the vapor pressure curve is known [38], a known and constant concentration can

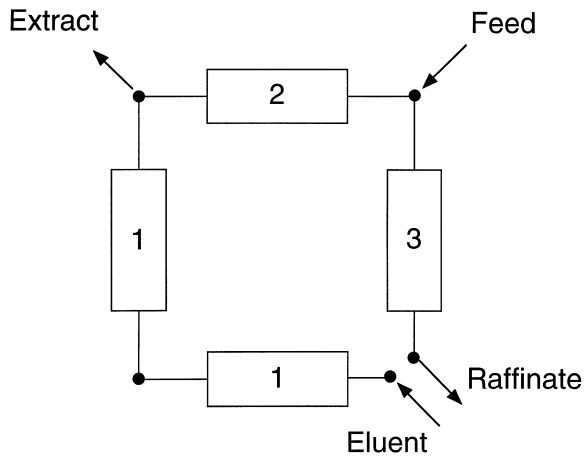


Fig. 4. Scheme of the connections between the columns in the GC–SMB unit, according to the adopted 2–1–1 configuration.

be obtained by saturating a nitrogen stream with enflurane at a given temperature. The saturation was performed in a stainless steel vessel that had partially been filled with enflurane and immersed in a thermostatted bath. For this a cryostat with ethanol as cooling medium was used. After passing through a cooling coil, nitrogen enters the vessel through a porous septum, in order to enhance mass transport. The concentration of racemic enflurane in the feed stream was checked by headspace capillary GC, using an enflurane–*n*-octane mixture of known composition as a calibration standard.

Enflurane enantiomers were collected from extract and raffinate streams through condensation in cooling traps using liquid nitrogen as cooling medium. After thawing, the liquid enantiomers were collected with two different syringes. The isolated enantiomers were characterized by chiral headspace capillary GC.

All flow-rates in the unit were adjusted by mass flow meters and controllers. These devices require a pressure drop of about 1 bar to be properly operated. During the SMB experiments the pressure was in the range of 1–2 bar at the outlet and 3–5 bar at the inlet of the unit.

## 3. Results and discussion

The results obtained in all the different steps involved in the development of a new SMB sepa-

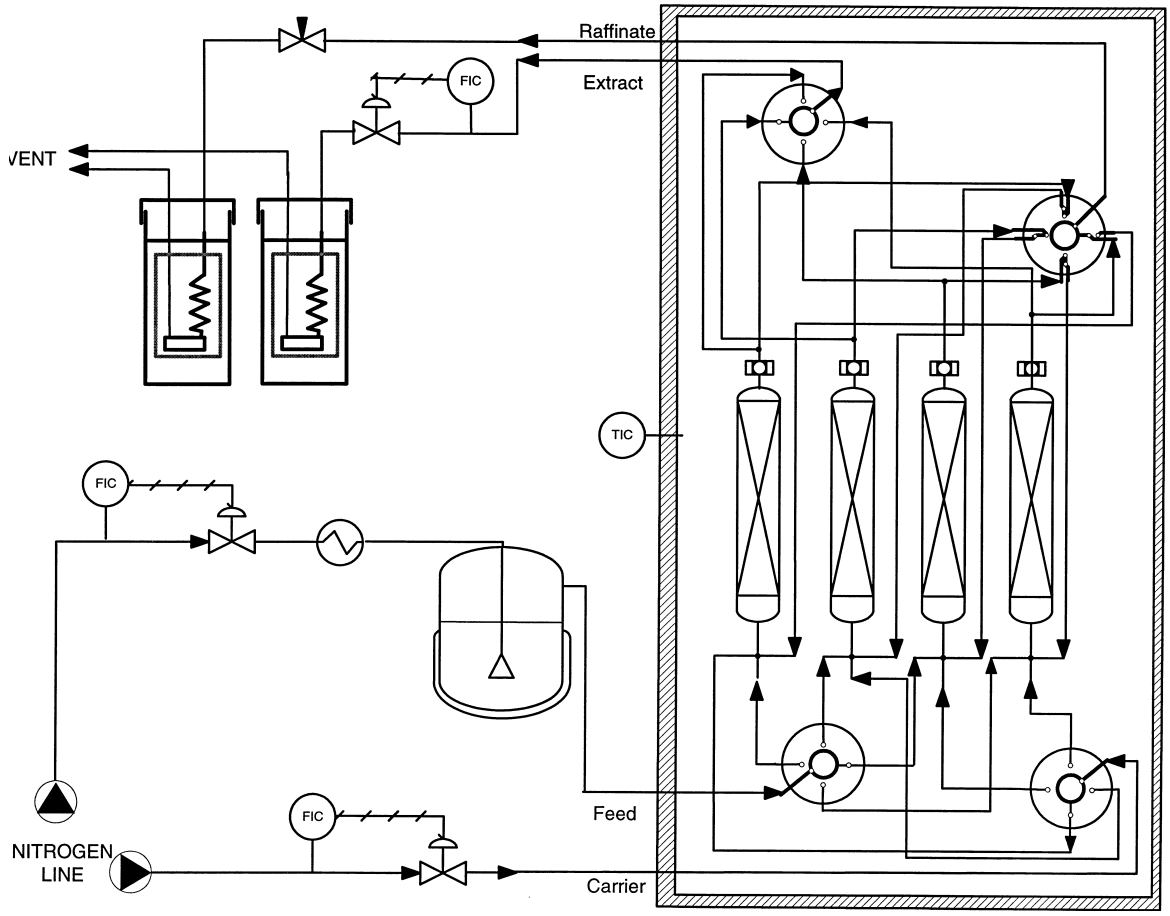


Fig. 5. Scheme of the laboratory scale GC–SMB unit.

ration are discussed separately: preparation of the stationary phase, characterization of the adsorption equilibria in the system, selection of the optimal operating conditions, operation of the SMB unit and analysis of the separation performance.

### *3.1. The chiral stationary phase*

The high melting point of cyclodextrin derivatives precludes their general use as an enantioselective stationary phase for chromatographic separations. Therefore, a solution of derivatized cyclodextrins in polysiloxanes is preferentially adopted [39]. Octakis(3-*O*-butanoyl-2,6-di-*O*-*n*-pentyl)-γ-cyclodextrin [11] dissolved in the apolar polysiloxane SE-54 [37] and coated on Chromosorb P AW DMCS [38] allows the enantiomer separation of the inhalation anesthetic enflurane in high chemical and enantiomeric purity by preparative GC.

The cyclodextrin derivative is prepared in a two-step synthesis. First, alkylation using *n*-pentyl bromide in dimethyl sulfoxide (DMSO) under basic conditions leads to a mixture of over- and under-dipentylated γ-cyclodextrin. The cyclodextrins in this mixture of isomers are preponderantly substituted in positions 2 and 6 of the glucose units. After chromatographic purification, in a second step, butanoylation with butyric anhydride in triethyl amine is easily achieved.

For preparative enantiomer separations, large quantities of the chiral selector are required. On the other hand, the isolation and purification of the

γ-cyclodextrin derivative is cumbersome and time-consuming. Previous results show that these purification procedures for cyclodextrin stationary phases are not always required and in some cases may even be detrimental to enantioselectivity [37]. We therefore employed the unpurified material, often referred to as a ''library'' of derivatives, consisting of the symmetrically substituted γ-cyclodextrin derivative (cf. Fig. 6 left) and of various isomers and homologues (Fig. 6 right) as determined by MALDI-TOF-MS [40]. Since *n*-pentyl and butanoyl moieties show only a marginal difference in mass, the degree of substitution has to be determined after isolation of the intermediate octakis(2,6-di-*O*-*n*-pentyl)-γ-cyclodextrin and not after the second step of the derivatization. Although the isolation of the symmetrically substituted compound is feasible, a mixture of the pentylated-γ-cyclodextrin derivatives (cf. Fig. 6 left and right, respectively) has been used since it also exhibits a good enantioselectivity. It is worth noting that even though the MALDI-TOF mass spectra cannot be a quantitative measure for the composition of the derivatized cyclodextrin batches, they clearly indicate a change in the substitution pattern of the cyclodextrin library, which allowed a reproducible up-scaling of the synthesis of the chiral selector to be employed in the pilot unit.

### *3.2. Characterization of the adsorption equilibrium*

The adsorption isotherms of the enflurane enantiomers on the cyclodextrin library dissolved in the non-polar polysiloxane SE-54 were determined using a pulse method, which requires the use of an appropriate model to process the experimental data. An ideal local equilibrium model was used, thus

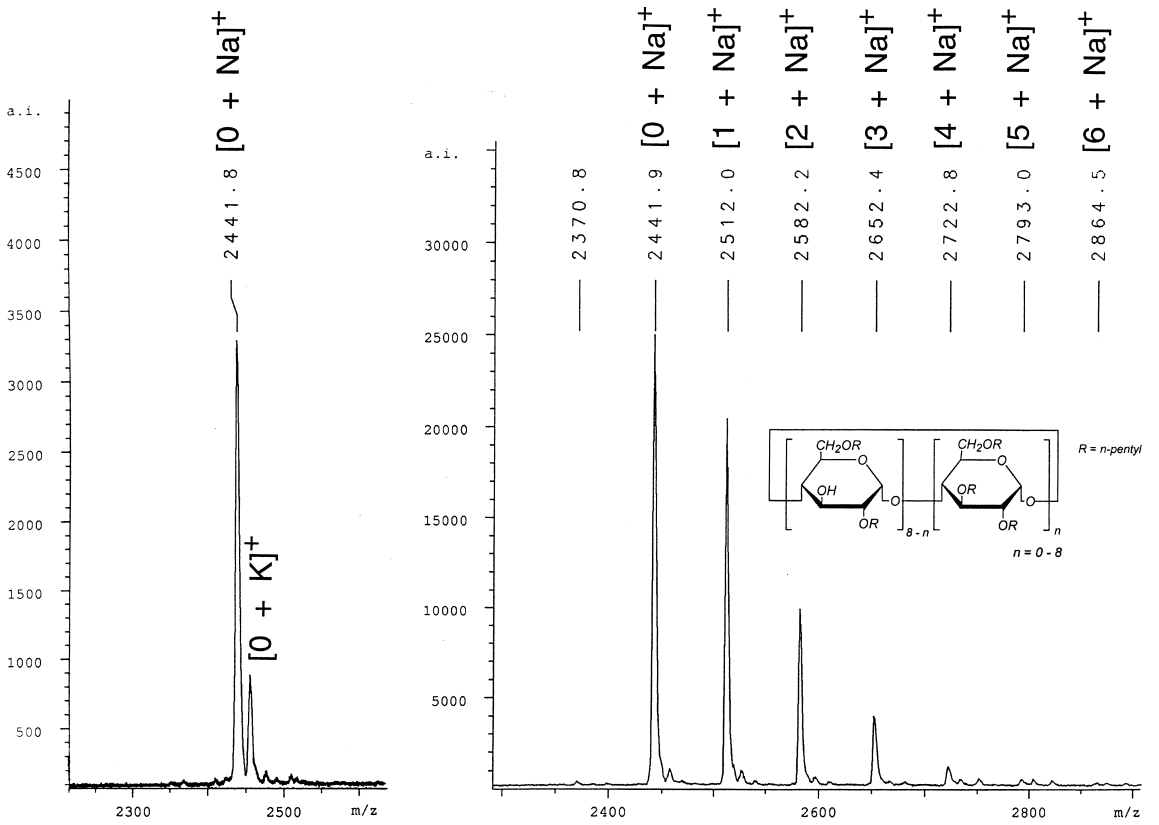


Fig. 6. MALDI-TOF mass spectra of octakis(2,6-di-*O*-*n*-pentyl)-γ-cyclodextrin; left: pure, right: mixture of isomers and homologues; all derivatives were detected as one-fold charged sodium and potassium ion adducts, number of 3-*O*-*n*-pentyl groups (*n*) is indicated.

neglecting axial dispersion and mass transfer resistance, but taking into account gas compressibility, pressure drop and sorption [41]. The mass balances of the adsorbate, i.e., the retained species, and of the non-retained carrier gas in a GC column can be written as:

$$\epsilon^* \frac{\partial c}{\partial t} + (1-\epsilon^*)\frac{\partial q}{\partial t} + \frac{\partial (vc)}{\partial z} = 0 \quad (1)$$

$$\epsilon^* \frac{\partial c_e}{\partial t} + \frac{\partial (vc_e)}{\partial z} = 0 \quad (2)$$

where $t$ is time, $z$ the axial coordinate of the column, $c$ the concentration of the retained species in the mobile phase, $q$ the concentration of the same species on the CSP, $c_e$ the concentration of the inert eluent i.e., nitrogen, in the fluid phase, $\epsilon^*$ the total void fraction and $v$ the superficial gas velocity. Introducing the molar fraction of the retained compound $y$ and assuming that the mobile phase behaves as an ideal gas, Eqs. (1) and (2) can be rewritten as follows:

$$\left[\epsilon^* + (1-\epsilon^*)\frac{\mathrm{d}q}{\mathrm{d}c}\right] p\frac{\partial y}{\partial t} + y\frac{\partial (pv)}{\partial z} + pv\frac{\partial y}{\partial z} = 0 \quad (3)$$

$$\frac{\partial (pvy)}{\partial z} = \frac{\partial (pv)}{\partial z} - \epsilon^* p\frac{\partial y}{\partial t} \quad (4)$$

where $p$ is the local pressure which remains constant in time. Combining Eqs. (3) and (4) yields:

$$\left[\epsilon^* + (1-\epsilon^*)(1-y)\frac{\mathrm{d}q}{\mathrm{d}c}\right]\frac{\partial y}{\partial t} + v\frac{\partial y}{\partial z} = 0 \quad (5)$$

This is a quasilinear homogeneous first-order partial differential equation and can be solved using the method of characteristics [42]. The retention time of each mole fraction value can be calculated by integrating Eq. (5) along the proper characteristic curve in the physical ($z$,$t$) plane:

$$t_R(y) = \int_0^L \frac{\epsilon^* + (1-\epsilon^*)(1-y)\dfrac{\mathrm{d}q}{\mathrm{d}c}}{v(z)}\mathrm{d}z \quad (6)$$

where $L$ is the column length. Along the integration path $y$ is constant because Eq. (5) is homogeneous.

This equation depends on the pressure profile in the column in two ways, i.e., through the velocity change along the column due to density/pressure variations and through slope of the isotherm $\mathrm{d}q/\mathrm{d}c$, since the concentration varies with pressure even at a constant mole fraction.

The first effect can be accounted for by using the Ergun equation for pressure drop in packed beds and assuming ideal gas phase behavior [43]. This allows to calculate the residence time of a non-retained species, $t_0$, for which $\mathrm{d}q/\mathrm{d}c = 0$ in Eq. (6), as a function of the outlet flow-rate and inlet and outlet pressure:

$$t_0 = \int_0^L \frac{\epsilon^*}{v(z)}\mathrm{d}z = \frac{V\epsilon^*}{Q_o}\frac{1}{J} \quad (7)$$

where $V$ is the volume of the column, $Q_o$ is the outlet volumetric flow-rate and $\epsilon^*$ is the total column void fraction. The parameter $J$, i.e., the James and Martin factor, which accounts for the pressure gradient [44,45], is defined as:

$$J = \frac{3}{2}\frac{(p_i/p_o)^2 - 1}{(p_i/p_o)^3 - 1} \quad (8)$$

where $p_i$ and $p_o$ are the inlet and outlet pressures, respectively. Eq. (7) was used to determine the total void fraction $\epsilon^*$ from injections of methane, which is assumed to be non-retained.

The effect of changes of $\mathrm{d}q/\mathrm{d}c$ at constant mole fraction due to the pressure gradient in the column can be accounted for by inserting an equation of state, e.g., the ideal gas law, in the equilibrium isotherm. Under very dilute conditions, $\mathrm{d}q/\mathrm{d}c = H$ does not depend on concentration and $(1\text{-}y) \approx 1$. Therefore, Eq. (6) can be integrated to provide the retention time of a linear pulse (analytical conditions), yielding the following relationship:

$$t_R = t_0\left(1 + \frac{1-\epsilon^*}{\epsilon^*}H\right) \quad (9)$$

where $H$ is the Henry constant of the adsorbate, i.e., the slope of its adsorption isotherm at infinite dilution. It is worth noting that this equation is formally identical to the one used in HPLC, i.e., under constant velocity conditions. This is due to the fact that the whole effect of the pressure gradient is accounted for by the value of $t_0$ calculated through Eqs. (7) and (8). The extension of this approach to

the case of non-linear adsorption equilibria is described later in Section 3.2.2.

### 3.2.1. Linear region

The Henry constants of both enantiomers have been calculated from the retention times, $t_R$, of appropriate pulses fed to a semi-preparative glass column containing the CSP described above. Headspace injections of 0.5 μl or less of racemic enflurane pulses yield peaks that are symmetrical and have retention times $t_R$ which are not dependent on the amount injected. This is the typical behavior of linear non-competitive isotherms and therefore Eq. (9) was used to determine the Henry constants, $H_i$, from the corresponding retention times, $t_{R,i}$. Notice that the indices A and B of the Henry constants $H_i$ refer to (*S*)-(+)-enflurane, i.e., the more retained enantiomer, and (*R*)-(−)-enflurane, the less retained enantiomer, respectively.

A temperature range between 29 and 60°C has been investigated and the temperature dependence of both Henry constants was interpolated through linear regression, according to the Van't Hoff equation. Experimental data are reported in Table 1 and shown in Fig. 7, together with their linear fits.

It is worth noting that, in agreement with previous findings [46], the Henry constants of each enantiomer, as well as enantioselectivity, defined as the ratio between the Henry constants, i.e., $\alpha = H_A/H_B$, increase when temperature decreases.

### 3.2.2. Non-linear region

The adsorption isotherms over a wider concentration range were determined at 40°C. This domain was chosen in order to cover the operating conditions of the SMB. Several pulse chromatograms were obtained by injecting increasing amounts of pure enantiomers, thus entering the non-linear equilibrium region, as indicated by the characteristic shape of the elution peaks shown in Fig. 8.

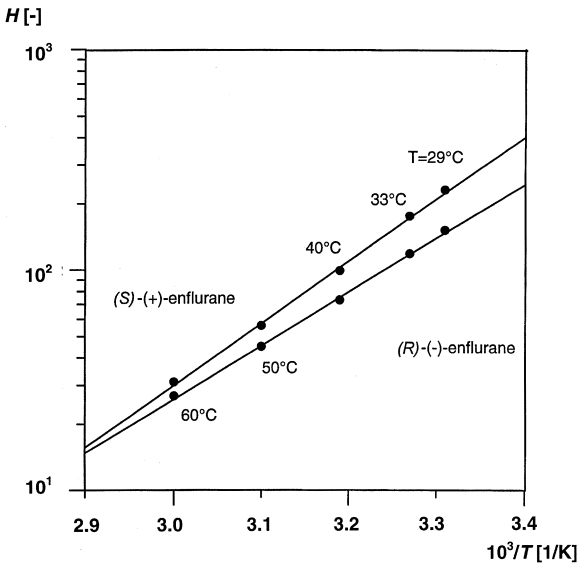


Fig. 7. Henry constants, $H_i$ (dimensionless), of the enflurane enantiomers vs. inverse temperature.

The observed retention times, $t_R$, of the peak maxima are related to flow conditions, injected amounts and adsorption isotherms through Eq. (6). In order to evaluate the integral on the right hand side of this equation we have to assume an adsorption isotherm model. The experimental data are shown in Fig. 9.

Since it is clear that a Langmuir model is not suitable to describe these data, the following modified Langmuir isotherm was used:

$$q_i = hc_i + \frac{g_i c_i}{1 + \sum_{j=1}^{2} k_j c_j} \quad (i = A, B) \tag{10}$$

where $c_i$ is the concentration in the mobile phase; $q_i$

Table 1
Experimental determination of the Henry constants

| $T$ (°C) | $Q$ (ml/s) | $P_i$ (bar) | $t_{R,B}$ (min) | $t_{R,A}$ (min) | $H_B$ | $H_A$ | Selectivity |
|---|---|---|---|---|---|---|---|
| 29 | 1.27 | 2.2 | 13.5 | 20.3 | 151 | 230 | 1.52 |
| 33 | 1.25 | 2.2 | 10.4 | 15.3 | 118 | 175 | 1.48 |
| 40 | 1.23 | 2.1 | 6.5 | 8.6 | 73 | 99 | 1.35 |
| 50 | 1.20 | 2.1 | 4.1 | 5.1 | 45 | 57 | 1.26 |
| 60 | 0.48 | 1.7 | 5.4 | 6.2 | 27 | 32 | 1.18 |

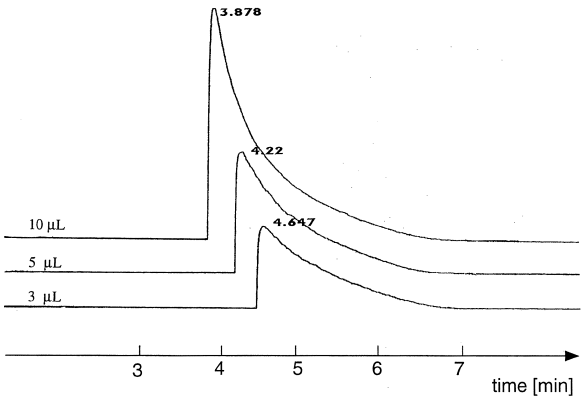


Fig. 8. Chromatograms obtained by injecting increasing amounts of the single pure (*R*)-(−)-enflurane enantiomer.

is the concentration in the stationary phase and $g_i$, $k_i$ and $h$ are the model parameters to be estimated.

Even though this model is empirical by nature, it is worth noting that in this case its two terms can well be justified physically. The behavior of the two enantiomers is in fact governed by two different retention mechanisms. On the one hand, the liquid SE-54 matrix coated on the solid support contributes non-enantioselectively to the overall gas uptake, while on the other hand ''enantioselective sites'' on the cyclodextrin molecules dissolved in the liquid phase are responsible for chiral recognition. As it can be seen in Fig. 9 the retention times, $t_R$, for the two enantiomers are almost the same for large injected amounts. Since the retention times at large injected amounts are essentially given by the linear term of the isotherm (Eq. (10)), they should be identical for the two enantiomers. Thus this part of the isotherm represents the non-enantioselective adsorption of the liquid SE-54 and of the support. On the other hand, the different retention times observed at low injected amounts are due to the enantioselective adsorption on the cyclodextrin molecules which are occupied preferentially by the (*S*)-(+)-enflurane, due to its stronger interaction [46]. This is taken into account by the selective Langmuir term of the isotherm model (Eq. (10)).

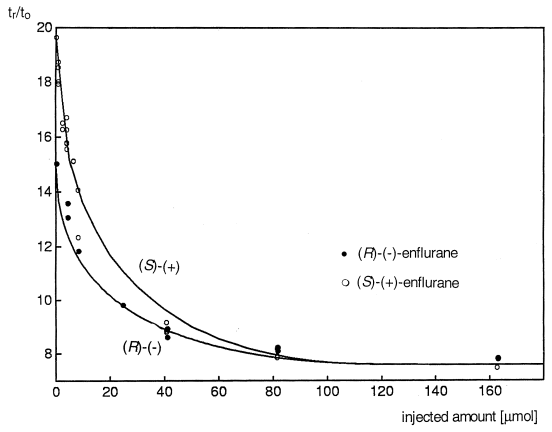


Fig. 9. Retention factor vs. injected amount for the two enantiomers of enflurane. Experimental data: (*R*)-(−)-enflurane (●) and (*S*)-(+)-enflurane (○); solid lines represent model results obtained through Eqs. (6) and (10).

The experimental values of the retention times of the two enantiomers are compared with those calculated using the modified Langmuir model (Eq. (10)) and Eq. (6) in Fig. 9. It is worth noting that the obtained agreement is satisfactory over a broad range of injected concentrations and flow-rates [47,48].

The estimated values of the model parameters are summarized in Table 2. As expected, the first eluted and therefore less retained enantiomer is (*R*)-(−)-enflurane, as indicated by the lower value of the selective coefficient $g_i$.

It is worth mentioning that the parameter estimation procedure can be significantly simplified by first determining the non-selective coefficient $h$ from the observed horizontal asymptote in the retention time/injected amount plot of Fig. 9. Next, the selective coefficient $g_i$ is calculated by considering that at infinite dilution conditions the isotherm (Eq. (10)) should reduce to the linear relation determined in Section 3.2.1, which implies:

$$g_i = H_i - h \tag{11}$$

Finally, the constant $k_i$ in the denominator in Eq. (10) is determined through a fitting procedure of the retention time measurements.

Table 2
Model parameters of the modified competitive Langmuir isotherm (Eq. (10)) for the adsorption equilibria of enflurane enantiomers on octakis(3-*O*-butanoyl-2,6-di-*O*-*n*-pentyl)-γ-cyclodextrin at 40°C

| | *h* | *g* | *k* (l/mmol) |
|---|---|---|---|
| (*R*)-(−)-Enflurane | 35 | 39 | 1.2 |
| (*S*)-(+)-Enflurane | 35 | 64 | 2.0 |

It should be noted that the loading capacity of the enantioselective ''sites'', given by the ratio $g_i/k_i$, is the same for both enantiomers. This confirms that they interact with the chiral selector by the same mechanism, although their affinities are different.

Recently, a related approach was used to describe the discrimination of the enantiomers of methyl lactate, methyl-2-chloropropionate and three inhalation anesthetics, among them enflurane, in the gas phase using thickness shear mode resonators [47]. The selective coating employed was the pure octakis(3-*O*-butanoyl-2,6-di-*O*-*n*-pentyl)-γ-cyclodextrin dissolved in various concentrations in a SE-54 polysiloxane matrix.

### *3.3. Design of GC–SMB operating conditions*

Optimal and robust operating conditions of SMB units under the assumption of constant fluid flow-rate in each section of the unit can be designed using appropriate criteria, obtained by applying a model based on equilibrium theory. These criteria have been derived for several non-linear isotherms of interest in applications [36,49,50]. In the case of linear isotherms this derivation becomes much simpler and can be extended also to the case where fluid flow-rate changes along the column cannot be neglected, as it is the case of GC–SMBs.

In order to achieve separation, in the second and in the third section of the unit, the flow-rates and the switch time have to satisfy the following inequalities:

$$t^{B}_{R,j} < t^{*} < t^{A}_{R,j} \quad (j = 2, 3) \tag{12}$$

This implies that the less retained component B initially present in the column is eluted before the next valve switch, while the more retained component A is not, hence it is retained in the stationary phase. This behavior actually describes the principle of SMB separation. Eqs. (7) and (9), can be used to evaluate the retention times under linear conditions, leading to:

$$t^{i}_{R,j} = \frac{V\epsilon^{*}}{Q_{o,j}J_j}\left(1 + \frac{1-\epsilon^{*}}{\epsilon^{*}}H_i\right) \tag{13}$$

where the James and Martin factor $J_j$ accounts for the effect of pressure drop on the flow-rate due to the compressibility of the gas phase. Using the equation above, the inequalities (Eq. (12)) lead to the constraints:

$$H_B < m_j < H_A \quad (j = 2, 3) \tag{14}$$

where:

$$m_j = \frac{Q_{o,j}t^{*}J_j - V\epsilon^{*}}{V(1-\epsilon^{*})} \tag{15}$$

The parameters $m_j$ can be regarded as the ratio between the flow-rates of the fluid and the solid phase in the equivalent counter-current unit. Note that this analysis is valid for both GC and HPLC; in the latter case $J_j = 1$ and $Q_o$ is constant along the column since the liquid phase is incompressible [49,51,52].

The constraints (Eq. (14)) identify in the operating parameter plane ($m_2$, $m_3$) a triangular complete separation region as shown in Fig. 10.

The separation performances of the unit in the different regions of the ($m_2$, $m_3$) plane indicated in Fig. 10, can be well explained with reference to Fig. 2 as follows. In the region above the triangle, i.e., where $m_2 > H_B$ but $m_3 > H_A$, a pure extract stream and an impure raffinate stream are obtained. In fact,

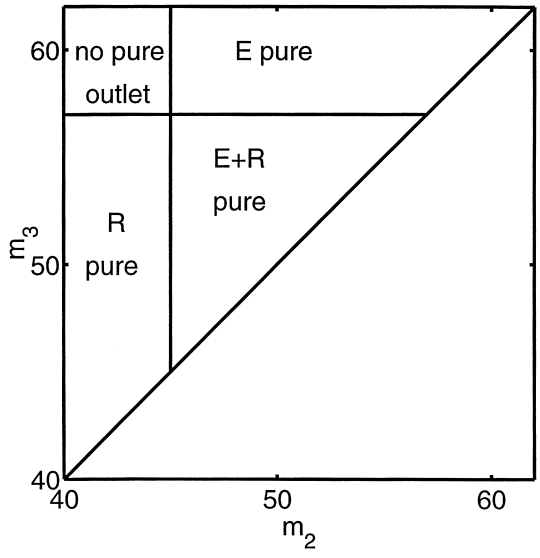


Fig. 10. Regions of the ($m_2$, $m_3$) plane with different separation performances, i.e., purities of the outlet streams, for a linear adsorption isotherm; $H_A = 57$, $H_B = 45$. Symbols E and R indicate extract and raffinate, respectively.

in that region $t^* > t^A_{R,3}$, so A is eluted from section 3 in the raffinate stream.

On the other hand, in the area to the left-hand side of the complete separation region, $m_3 < H_A$ but $m_2 < H_B$. Under these conditions the raffinate stream is pure but, being $t^* < t^B_{R,2}$, B is not completely eluted from the CSP in section 2. So B is carried by the CSP to section 1, and then eluted in the extract stream, which is then not pure.

In the ''no pure outlet'' region both streams are impure, because $t^* > t^A_{R,3}$ and $t^* < t^B_{R,2}$. Inequalites (Eq. (14)) are valid only under linear conditions, i.e., using a very diluted feed stream. However, as mentioned above, in liquid phase units or low pressure drop gas phase units the complete separation region in the ($m_2$, $m_3$) plane can be calculated also for non-linear conditions. The effect of non-linearity consists qualitatively in a change in shape and position of the complete separation region, such as that illustrated in Fig. 11. Since the eluent is not adsorbable, the triangle is deformed toward the lower left-hand corner of the ($m_2$, $m_3$) plane [49,51,52]; the greater the racemate feed concentration the larger the deformation of the complete separation region. We

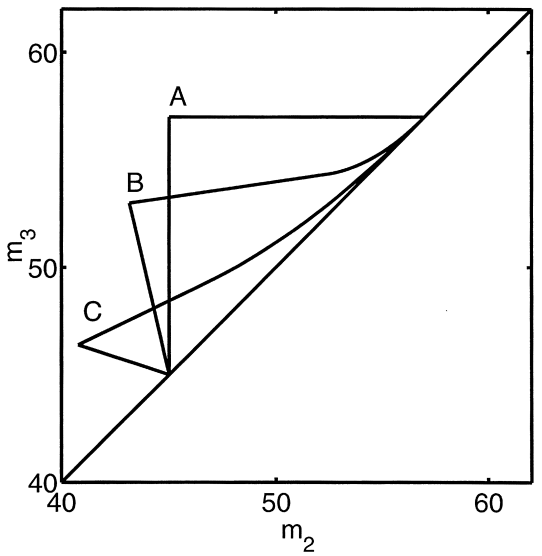


Fig. 11. Effect of the racemate concentration in the feed stream on the complete separation region in the ($m_2$, $m_3$) plane. Parameters of the isotherm model (Eq. (10)): $h=0$, $g_A=57$, $k_A=2$, $g_B=45$, $k_B=1.2$; region (A): $c^F_T \to 0$, region (B): $c^F_T=0.05$ mmol/l; region (C): 0.2 mmol/l.

expect the qualitative behavior for a gas phase unit with significant pressure drop to be the same, even though in this case predictive calculations are not yet possible.

### 3.4. GC–SMB experimental results

The experiments performed with the GC–SMB pilot unit were designed to demonstrate the feasibility of the GC–SMB continuous separation of enflurane by determining the shape and location of the complete separation region in the operating parameter space ($m_2$, $m_3$). This is to our knowledge the first application of the GC–SMB technology to chiral separations.

The experimental operating conditions were designed on the basis of the following arguments: previous theoretical findings indicate that the feed concentration of the components to be separated is a key factor in determining the efficiency of the separation, as well as its robustness. Increasing feed concentration yields larger productivity but lower robustness, hence the best choice of feed concentration represents a compromise between these two opposite needs [36]. Therefore, it is very important to know the non-linear effect associated with the increase of feed concentration, which leads to a distortion of the complete separation region (see Fig. 11). In the case of HPLC–SMB units, where velocity variations of the mobile phase are negligible, this effect can be predicted quantitatively; on the contrary, a non-linear theory is not yet available in the case of GC–SMBs where velocity changes are significant and the non-linear effect must be investigated experimentally.

Therefore, two sets of experiments have been performed, all at the same temperature, $T=50$°C, but at two different feed concentration levels, as shown in Table 3. In all cases, the linear complete separation region has been taken as a reference location for the actual non-linear one; the linear triangle is the square triangle whose base points on the diagonal correspond to the Henry constants of the two enantiomers at the operating temperature, i.e., $H_B=45$ and $H_A=57$ (cf. Table 1). In order to investigate how the complete separation region is distorted due to the chosen feed concentration, it is convenient to run a set of experiments with operating conditions corre-

Table 3
Operating conditions and separation performances of the experimental runs

| Run | Feed racemate concentration (%) | $t^*$ (min) | $m_1$ | $m_2$ | $m_3$ | ee extract (%) | ee raffinate (%) |
|---|---|---|---|---|---|---|---|
| A | 0.8 | 6 | 105 | 45 | 57 | 70 | 66 |
| B | 0.8 | 6.5 | 114 | 49 | 64 | 88 | 10 |
| C | 0.8 | 5 | 86 | 37 | 49 | 28 | 92 |
| D | 1.6 | 5 | 86 | 37 | 47 | 56 | 52 |
| E | 1.6 | 6 | 105 | 45 | 57 | 90 | 12 |
| F | 1.6 | 4.5 | 77 | 33 | 43 | 18 | 96 |

sponding to operating points located along a straight line crossing the linear triangle. This can be done by keeping the flow-rates in all experiments constant and changing only the switch time, as it can be readily seen from Eq. (15). The experimental values of the flow-rates are in all experiments: $Q_1 = Q_D =$ 1.3 Nl/min; $Q_2 = 0.49$ Nl/min; $Q_3 = 0.54$ Nl/min; $Q_F = 0.05$ Nl/min; $Q_E = 0.81$ Nl/min; $Q_R = 0.54$ Nl/min (D for the eluent inlet, F for the feed stream, E and R for the extract and raffinate streams, respectively). The pressure levels correspond to values of the James and Martin factor (Eq. (8)) between 0.87 and 0.93.

The switch time and the flow-rate ratios of the experimental runs calculated through Eq. (15) are reported in Table 3; the corresponding operating points in the ($m_2$, $m_3$) plane are shown in Fig. 12, together with the linear complete separation region. The positions of operating points A, B and C (with a feed concentration of 0.8%) and that of points D, E and F (where the feed concentration is 1.6%) must be compared to two different complete separation regions (cf. Fig. 11). The last two columns in Table 3 report the enantiomeric excess measured in the raffinate and extract streams for each experimental run. It is worth recalling the definition of the parameters through which the purity of the outlet streams can be measured. The most common definition in SMB applications is that of purity of the product streams:

$$P_E = \frac{c_A^E}{c_A^E + c_B^E} \cdot 100 \tag{16}$$

$$P_R = \frac{c_B^R}{c_A^R + c_B^R} \cdot 100 \tag{17}$$

however, in the case of chiral separations the % enantiomeric excess reported in Table 3 is most often used:

$$ee_E = \frac{c_A^E - c_B^E}{c_A^E + c_B^E} \cdot 100 \tag{18}$$

$$ee_R = \frac{c_B^R - c_A^R}{c_A^R + c_B^R} \cdot 100 \tag{19}$$

It follows that the two sets of parameters are related by the following equations:

$$P_E = (100 + ee_E)/2 \tag{20}$$

$$P_R = (100 + ee_R)/2 \tag{21}$$

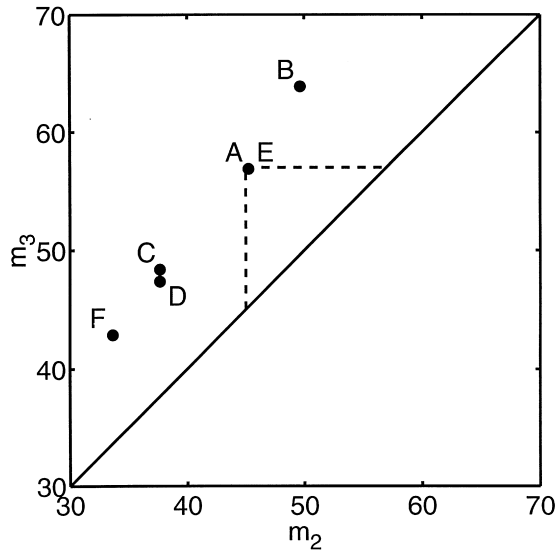


Fig. 12. Comparison of the predicted linear region of complete separation in the ($m_2$, $m_3$) plane with the operating points (●) of the experimental runs reported in Table 3.

First, let us consider the three experiments, A, B and C, performed at low concentration. It can be readily observed that in run A, whose operating point coincides with the optimal point of the linear complete separation region, relatively high purity in both product streams has been achieved ($ee_E = 70\%$ and $ee_R = 66\%$, corresponding to $P_E = 85\%$ and $P_R = 83\%$). This indicates that point A is outside the actual non-linear complete separation region corresponding to the feed concentration of 0.8%, but it is not too far from it. This is confirmed by the results obtained in runs B and C; in fact in run B the quality of the extract product is much better than that of the raffinate ($ee_E = 86\%$ and $ee_R = 10\%$, i.e., $P_E = 94\%$ and $P_R = 55\%$), whereas in run C the opposite is observed ($ee_E = 28\%$ and $ee_R = 92\%$, i.e., $P_E = 64\%$ and $P_R = 96\%$). These results are consistent with the position of the operating points B and C in Fig. 12, with respect to the position of point A (cf. Fig. 12 with the separation regions illustrated in Fig. 10). Thus summarizing, these results indicate that at 0.8% of feed concentration, the actual non-linear complete separation region is similar to the linear one, thus indicating a low degree of overloading of the SMB columns.

Let us consider the second set of experiments: D, E and F. In this case, run D is the one where the best separation performances in both outlet streams have been achieved ($ee_E = 56\%$ and $ee_R = 52\%$, corresponding to $P_E = 78\%$ and $P_R = 76\%$). As in the case of run A, this suggests that point D gives a good indication of the location of the optimal point of the actual non-linear complete separation region corresponding to 1.6% of feed concentration. Therefore the shift from point A to point D is representative of the change of shape and location of the complete separation region due to the increase from 0.8% to 1.6% of feed concentration. This is qualitatively consistent with the theoretical findings briefly summarized in the previous section and illustrated in Fig. 11 and it indicates a strong non-linear overloading effect occurring when doubling the feed concentration from 0.8% to 1.6%. This is further confirmed by the experimental runs E and F, for which the same comments as for runs B and C can be repeated (run E: $ee_E = 90\%$ and $ee_R = 12\%$, i.e., $P_E = 95\%$ and $P_R = 56\%$; run F: $ee_E = 18\%$ and $ee_R = 96\%$, i.e., $P_E = 59\%$ and $P_R = 98\%$). It is worth noting that in all runs in which one outlet stream is very pure, i.e., runs B, C, E and F, the collected amounts of the very pure stream are rather small, as can be readily seen from material balance considerations.

## 4. Concluding remarks

As with any other separation process, the operation of SMB units has to be considered in terms of purity performances and productivity, since both these parameters are of key importance to evaluate the economic value of the process. In this work we have demonstrated the feasibility of the separation of the volatile inhalation anesthetic enflurane by GC–SMB, i.e., the possibility of achieving high purity performances. However, such high purities were achieved only in one outlet stream at a time, while complete separation, i.e., enantiomeric excess greater than 90% in both outlet streams, has never been obtained. On the other hand, the maximum productivity achieved in the performed experimental runs (at 1.6% feed concentration) is about 0.01 g of enantiomers per gram of stationary phase per day. This is probably a satisfactory productivity for many applications, but is certainly not a typical value for this kind of technology. We expect that the separation performance, both in terms of purity and productivity, could be significantly improved by operating the unit at a temperature lower than 50°C, which represents the minimum value achievable with the current set-up. This is due to the increase in selectivity which, as it can be seen from the data in Fig. 7 increases for example from 1.26 at 50°C to 1.5 at 30°C.

Besides the actual separation performances achieved, the analysis performed in this work demonstrates that, by properly operating on the flow-rate ratios $m_2$ and $m_3$, we are in the position of driving the separation performances of GC–SMB units toward the desired specifications. In the absence of a quantitative theory, this has been achieved only in qualitative terms, i.e., by providing guidelines about how to change the units flow-rates so as to satisfy the given specifications. The reliability of these conclusions is demonstrated by the experimental results reported in this work.

## 5. List of symbols

| | |
|---|---|
| $c$ | concentration |
| ee | enantiomeric excess |
| $g$ | isotherm parameter (cf. Eq. (10)) |
| $h$ | isotherm parameter (cf. Eq. (10)) |
| $H$ | Henry constant |
| $J$ | James and Martin factor |
| $k$ | isotherm parameter (cf. Eq. (10)) |
| $L$ | column length |
| $m$ | SMB operating parameter |
| $p$ | local pressure |
| $P$ | purity |
| $q$ | concentration of a retained species in the CSP |
| $Q$ | volumetric flow-rate |
| $t$ | time |
| $t_R$ | retention time |
| $t_0$ | residence time of a non-retained species |
| $t^*$ | switch time |
| $v$ | superficial gas velocity |
| $V$ | column volume |
| $y$ | column volume |
| $z$ | axial coordinate |

### 5.1. Greek letters

| | |
|---|---|
| $\alpha$ | enantioselectivity |
| $\epsilon^*$ | total void fraction |

### 5.2. Subscripts and superscripts

| | |
|---|---|
| A | more retained component |
| B | less retained component |
| D | desorbent stream, i.e., eluent inlet |
| e | non-retained eluent |
| E | extract stream |
| F | feed stream |
| i | column inlet |
| o | column outlet |
| R | raffinate stream |

## Acknowledgements

The authors thank the Wacker Chemie, Munich, Germany, for a generous gift of γ-cyclodextrin and M. Preschel, Universität Tübingen, Germany, for the preparation of enantiomerically pure enflurane samples. M.J. thanks the Deutscher Akademischer Austauschdienst for a short-term scholarship. Part of the experimental activity was carried out at the Politecnico di Milano, Milan, Italy. We thank Dr. Davino Gelosa and Andrea Sliepcevich for their technical advice.

## References

[1] A.C. Hall, W.R. Lieb, N.P. Franks, Br. J. Pharmacol. 906 (1994) 112.
[2] B. Dickinson, N.P. Franks, W.R. Lieb, Biophys. J. 2019 (1994) 66.
[3] N.P. Franks, W.R. Lieb, Nature 607 (1994) 367.
[4] N.P. Franks, W.R. Lieb, Science 427 (1991) 254.
[5] B.D. Harris, E.J. Moody, A.S. Basile, P. Skolnick, Eur. J. Pharmacol. 269 (1994) 267.
[6] E.J. Moody, B.D. Harris, P. Skolnick, Brain Res. 101 (1993) 615.
[7] R.C. Terell, US Pat. 3 469 011 (1969).
[8] R.C. Terell, US Pat. 3 527 813 (1970).
[9] J. Meinwald, W.R. Thompson, D.L. Pearson, W.A. König, T. Runge, W. Francke, Science 251 (1991) 560.
[10] K.J. Garton, P. Yuen, J. Meinwald, K.E. Thummel, E.D. Kharasch, D. Evan, Drug Metab. Dispos. 23 (1995) 1426.
[11] W.A. König, R. Krebber, P. Mischnick, J. High Resolut. Chromatogr. 12 (1989) 732.
[12] V. Schurig, H. Grosenick, B.S. Green, Angew. Chem., Int. Ed. Engl. 32 (1993) 1662.
[13] V. Schurig, H. Grosenick, J. Chromatogr. A 666 (1994) 617.
[14] V. Schurig, B.S. Green, H. Grosenick, German Offenlegungsschrift, P 4317139.7 (1994).
[15] A. Shitangkoon, D.U. Staerk, G. Vigh, J. Chromatogr. A 657 (1993) 387.
[16] D.U. Staerk, A. Shitangkoon, G. Vigh, J. Chromatogr. A 663 (1994) 79.
[17] D.U. Staerk, A. Shitangkoon, G. Vigh, J. Chromatogr. A 677 (1994) 133.
[18] R.M. Nicoud, LC·GC Int. 5 (1992) 43.
[19] R.M. Nicoud, G. Fuchs, P. Adam, M. Bailly, E. Küsters, F.D. Antia, R. Reuille, E. Schmid, Chirality 5 (1993) 267.
[20] E. Küsters, G. Gerber, F.D. Antia, Chromatographia 40 (1995) 387.
[21] E. Francotte, P. Richert, J. Chromatogr. A 769 (1997) 101.
[22] M. Negawa, F. Shoji, J. Chromatogr. 590 (1992) 113.
[23] C.B. Ching, B.G. Lim, E.J.D. Lee, S.C. Ng, J. Chromatogr. 634 (1993) 215.
[24] F. Charton, R.M. Nicoud, J. Chromatogr. A 702 (1995) 97.
[25] N. Gottschlich, S. Weidgen, V. Kasche, J. Chromatogr. A 719 (1996) 267.
[26] S. Nagamatsu, K. Murazumi, H. Matsumoto, S. Makino, Proceedings of the Chiral Europe '96 Symposium, Spring Innovations, Stockport, UK, 1996, p. 97.

[27] E. Cavoy, M.F. Deltent, S. Lehoucq, D. Miggiano, J. Chromatogr. A 769 (1997) 49.
[28] N. Gottschlich, V. Kasche, J. Chromatogr. A 765 (1997) 201.
[29] D.W. Guest, J. Chromatogr. A 760 (1997) 159.
[30] L.S. Pais, J.M. Louriero, A.E. Rodrigues, Chem. Eng. Sci. 52 (1997) 245.
[31] M. Schulte, R. Ditz, R.M. Devant, J. Kinkel, F. Charton, J. Chromatogr. A 769 (1997) 93.
[32] M.P. Pedeferri, G. Zenoni, M. Mazzotti, M. Morbidelli, Chem. Eng. Sci., (1998) submitted for publication.
[33] J.Y. Clavier, R.M. Nicoud, M. Perrut, in: High Pressure Chemical Engineering, Elsevier, London, 1996.
[34] G. Storti, M. Mazzotti, L.T. Furlan, M. Morbidelli, S. Carrà, Sep. Sci. Technol. 27 (1992) 1889.
[35] M. Mazzotti, R. Baciocchi, G. Storti, M. Morbidelli, Ind. Eng. Chem. Res. 35 (1996) 2313.
[36] M. Mazzotti, G. Storti, M. Morbidelli, J. Chromatogr. A 769 (1997) 3.
[37] V. Schurig, H. Grosenick, M. Juza, Recl. Trav. Chim. Pays-Bas 114 (1995) 211.
[38] M. Juza, E. Braun, V. Schurig, J. Chromatogr. A 769 (1997) 199.
[39] V. Schurig, H.P. Nowotny, J. Chromatogr. 441 (1988) 155.
[40] B. Chankvetadze, G. Endresz, G. Blaschke, M. Juza, H. Jakubetz, V. Schurig, Carbohydr. Res. 287 (1996) 139.
[41] J.R. Conder, C.L. Young, Physicochemical Measurements by Gas Chromatography, Wiley, Chichester, 1979, Ch. 9.
[42] A. Varma, M. Morbidelli, Mathematical Methods in Chemical Engineering, Oxford University Press, New York, Oxford, 1997, Ch. 6.
[43] S. Ergun, Chem. Eng. Prog. 48 (1952) 89.
[44] D.H. Everett, Trans. Faraday Soc. 61 (1965) 1637.
[45] D.U. Staerk, A. Shitangkoon, E. Winchester, G. Vigh, A. Felinger, G. Guiochon, J. Chromatogr. A 734 (1996) 155.
[46] V. Schurig, M. Juza, J. Chromatogr. A 757 (1997) 119.
[47] K. Bodenhöfer, A. Hierlemann, M. Juza, V. Schurig, H. Göpel, Anal. Chem. 69 (1997) 4017.
[48] S. Jacobson, S.G. Shirazi, G. Guiochon, AIChE J. 37 (1991) 836.
[49] G. Storti, M. Mazzotti, M. Morbidelli, S. Carrà, AIChE J. 39 (1993) 471.
[50] A. Gentilini, C. Migliorini, M. Mazzotti, M. Morbidelli, J. Chromatogr. A 805 (1998) 37.
[51] M. Mazzotti, G. Storti, M. Morbidelli, AIChE J. 40 (1994) 1825.
[52] M. Mazzotti, G. Storti, M. Morbidelli, AIChE J. 42 (1996) 2784.